

## High current density field emission from arrays of carbon nanotubes and diamond-clad Si tips

F. G. Tarntair, L. C. Chen, S. L. Wei, W. K. Hong, K. H. Chen, and H. C. Cheng

Citation: *Journal of Vacuum Science & Technology B* **18**, 1207 (2000); doi: 10.1116/1.591362

View online: <http://dx.doi.org/10.1116/1.591362>

View Table of Contents: <http://scitation.aip.org/content/avs/journal/jvstb/18/3?ver=pdfcov>

Published by the AVS: Science & Technology of Materials, Interfaces, and Processing

---

### Articles you may be interested in

[Modeling of emitted current distribution and electron trajectories in the thin-film field-emission triode](#)  
*J. Vac. Sci. Technol. B* **22**, 1250 (2004); 10.1116/1.1736636

[Direct growth of aligned carbon nanotube field emitter arrays onto plastic substrates](#)  
*Appl. Phys. Lett.* **83**, 4661 (2003); 10.1063/1.1630167

[Collective emission degradation behavior of carbon nanotube thin-film electron emitters](#)  
*Appl. Phys. Lett.* **79**, 1036 (2001); 10.1063/1.1392982

[Large current density from carbon nanotube field emitters](#)  
*Appl. Phys. Lett.* **75**, 873 (1999); 10.1063/1.124541

[Electron field emission from diamond grown by a multiple pulsed laser process](#)  
*J. Vac. Sci. Technol. B* **16**, 1184 (1998); 10.1116/1.590029

---

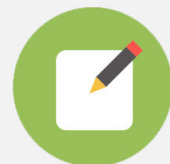


## Re-register for Table of Content Alerts

Create a profile.



Sign up today!



# High current density field emission from arrays of carbon nanotubes and diamond-clad Si tips

F. G. Tarntair

*Department of Electronics Engineering and Institute of Electronics, National Chiao Tung University, Hsinchu, Taiwan*

L. C. Chen and S. L. Wei

*Center for Condensed Matter Sciences, National Taiwan University, Taipei, Taiwan*

W. K. Hong

*Department of Electronics Engineering and Institute of Electronics, National Chiao Tung University, Hsinchu, Taiwan*

K. H. Chen

*Institute of Atomic and Molecular Sciences, Academia Sinica, Taipei, Taiwan*

H. C. Cheng

*Department of Electronics Engineering and Institute of Electronics, National Chiao Tung University, Hsinchu, Taiwan*

(Received 6 January 2000; accepted 3 March 2000)

Arrays of carbon nanotubes (CNT) and diamond-clad Si tips were grown by microwave plasma-enhanced chemical vapor deposition. The former ones were grown directly on prepatterned cobalt-coated silicon substrate, while the latter ones were grown on Si-tip arrays. Each array contains  $50 \times 50$  emitting cells and each individual cell is  $3 \mu\text{m}$  square. A maximum effective emission current density of about  $17 \text{ A/cm}^2$  (at a macroscopic field of  $17.5 \text{ V}/\mu\text{m}$ ) has been demonstrated, while a macroscopic emission current density of  $10 \text{ mA/cm}^2$  with operating fields around  $10 \text{ V}/\mu\text{m}$  can be routinely achieved from an array of CNT emitters. In contrast, operating fields above  $20 \text{ V}/\mu\text{m}$  were needed to draw a comparable emission current density from all of the diamond-clad Si tips arrays. Emission stability test performed at  $40 \text{ mA/cm}^2$  for CNT arrays also showed little sign of degradation. Due to the high efficiency of electron emission, simple sample process, and large area growth capability, field emitter arrays based on CNT are attractive for flat panel display applications. © 2000 American Vacuum Society. [S0734-211X(00)08003-3]

## I. INTRODUCTION

A key technology of vacuum microelectronics is the fabrication of field emitter arrays for operating as cold cathodes, of which the potential applications include the electron sources of ultrathin flat-panel field emission display (FED), microsensors, nanoprobe of atomic force microscopy (AFM) or scanning tunneling microscope (STM) and micro-sized intense electron sources.<sup>1-4</sup> In order to achieve high electron emission at low voltage for cold cathode operation, the choice of a cathode material with low work function and/or producing fine sharp features are indispensable. Among the various types of field emitters, carbon-based materials, such as diamond, diamond-like-carbon, and carbon nanotube (CNT), have gained a considerable attention owing to their unique electronic, mechanical, and chemical properties. Initial promise of diamond has been hampered to transfer to practical cathode application for two reasons. First, the chemical vapor deposition process for diamond is usually carried out at high temperatures. Second, although the turn-on field is low, emission current densities above  $\mu\text{A/cm}^2$  cannot be obtained at low electric fields due to the high resistance of bulk diamond film,<sup>5,6</sup> an inherent wide-band-gap property. In view of this, carbon nanotubes and amorphous forms of carbon are in many ways better suited

for display applications than diamond. The following three advantages are notable. (i) They can be fabricated using chemical vapor deposition (CVD) or physical vapor deposition (PVD) at low temperatures. (ii) Their structures are easily made in nanometer-scale forms, which avoids the complications of manufacturing geometric features. (iii) They have higher electron conductivity than diamond.

Indeed, several groups<sup>7-13</sup> have already demonstrated excellent field emission properties of CNT. The reported current densities were in the range of  $0.1-100 \text{ mA/cm}^2$ . In most studies, randomly distributed carbon nanotubes were grown by laser ablation or by arc discharge technique, the most commonly used method up until now. Fabrication of cathodes for field emission involves their separation and purification from a carbon powder deposit and subsequent mounting or encapsulation. These post-growth processes inevitably bring in some technological limitation to the use of CNT. Array of well-aligned nanotubes directly deposited on Fe-coated porous Si substrate has also been demonstrated recently.<sup>14</sup> Quite surprisingly, the electron emission properties of these self-oriented CNT blocks and towers were not improved over those of CNT emitters assembled without alignment. Preferential electron emission from the edge of the well-aligned CNT blocks was observed when the number density of CNT within each block was very high. Presum-

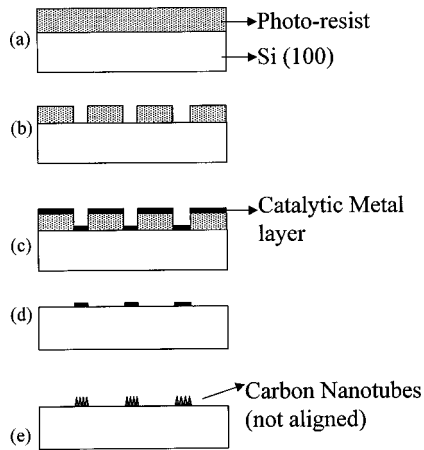


FIG. 1. Schematic sketch of the fabrication process of CNT array (a) photoresist coated on Si substrate, (b) lithographic pattern definition, (c) cobalt metal layer deposition, (d) photoresist lift off with ACE, then the array of  $50 \times 50$  cells was formed, (e) CNT arrays formed by MPECVD.

ably, reduction in the enhancement of local field may occur as the intertube distance approaches zero.

In this report, we present a straightforward technique for fabricating CNT arrays with no post-growth process. Since small array size with high density of emitting cells is desirable for improved resolution in display devices, lithographic technique was employed to produce arrays containing  $50 \times 50$  emitting cells of  $3 \mu\text{m} \times 3 \mu\text{m}$  square shape. The CNT were then grown directly on the cobalt-coated patterned substrate by microwave plasma-enhanced chemical vapor deposition. Our field emission data demonstrates that CNT arrays exhibited a large current density, which routinely exceeded  $1 \text{ A/cm}^2$ , at moderate field. Such high current density is necessary for many applications: for instance, flat-panel FED requires  $10 \text{ mA/cm}^2$ , whereas microwave power amplifier demands at least  $500 \text{ mA/cm}^2$ .<sup>13</sup> Emission stability of CNT as well as comparison with various arrays of diamond-clad Si tips are also presented.

## II. EXPERIMENTS

The fabrication procedure of carbon nanotube emitter array is shown schematically in Figs. 1(a)–1(e). As shown in Figs. 1(a) and 1(b), a  $1\text{-}\mu\text{m}$ -thick photoresist was spin coated on a *p*-type Si(100) substrate and a  $50 \times 50$  array of  $3 \mu\text{m}$  square cells at  $10 \mu\text{m}$  pitch was patterned by photolithography. Then, a thin cobalt layer ( $\sim 30 \text{ nm}$ ) was coated directly on the photoresist patterned Si substrate by electron beam evaporation, Fig. 1(c). An array of Co cells was thus formed after the photoresist was removed by lift-off method as depicted in Fig. 1(d). Finally, carbon nanotubes were grown selectively on Co cells by microwave plasma-enhanced chemical vapor deposition.  $\text{CH}_4$ ,  $\text{N}_2$ , and  $\text{H}_2$  were used as the source gases and typical flow rates were 20, 80, and 80 sccm, respectively. The microwave power was kept at 1.5 kW and the chamber pressure was kept in 50 Torr. The substrate temperature during growth was estimated at about  $600^\circ\text{C}$  and typical deposition time was 20 min.

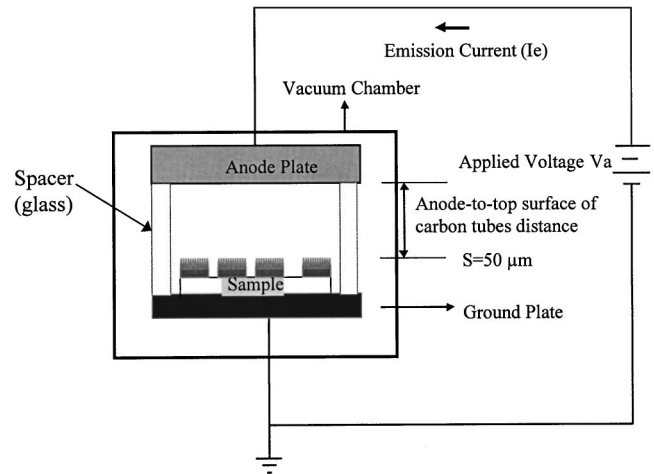


FIG. 2. Schematic diagram of a high vacuum system for field emission measurement.

Auger electron spectroscopy (AES) was performed to determine the chemical contents in tubes. Field emission properties were characterized in a high vacuum environment with a base pressure of about  $8.0 \times 10^{-8}$  Torr (Fig. 2). The copper anode plate was positioned  $30 \mu\text{m}$  above the emitter surface. Field emission characterization can be obtained from the emitter array over a voltage sweep from 0 to 1100 V.

## III. RESULTS AND DISCUSSION

Figure 3(a) shows a typical photograph of an array of CNT emitters. It can be seen that CNT grew only on the

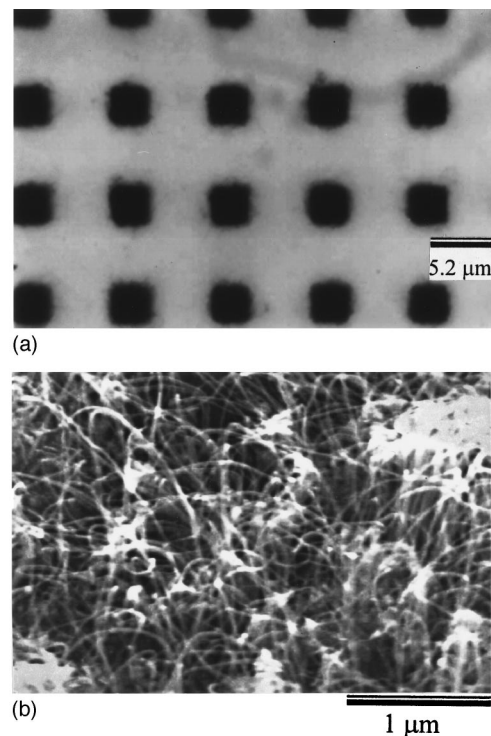


FIG. 3. (a) Plain view of CNT array imaged by optical microscopy at  $1000 \times$ . (b) Typical SEM micrograph of CNT inside a cell.

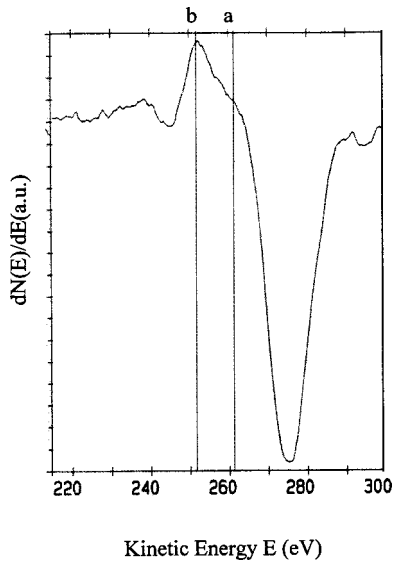


FIG. 4. Typical Auger spectrum of CNT, the shoulder (peak a and peak b) suggests that the surface structure is close to graphitic carbon.

patterned catalytic metal cells in the array but not on the plain Si substrate. Furthermore, no intercell connection of tubes was observed. Scanning electron microscopy (SEM) studies reveal that our carbon nanotubes are 20–30  $\mu\text{m}$  in length and about 60–70 nm in diameter. As shown in Fig. 3(b), the density of carbon nanotubes in each cell was very high. However, no correlation in the orientation of nanotubes was observed.

It should be mentioned that only carbon element was observed in the nanotubes even though nitrogen was employed during CVD growth. However, nitrogen addition in the gas phase appears to promote the formation of CNT, in that, the growth rate of carbon nanotubes was very low if no nitrogen gas was introduced during the deposition. Figure 4 depicts a typical Auger spectrum of the nanotube. In addition to the main carbon peak at 272 eV, the low energy shoulder around 258–260 and 248–250 eV can clearly be seen in the AES spectrum, confirming the graphite sheet-like structure of the nanotubes.

For field emission study, several samples have been tested. While  $I$ – $V$  curves were found to vary somewhat from sample to sample, they all exhibited high current at low operating voltages. Typical anode current ( $I$ ) versus applied voltage ( $V$ ) for an array of the CNT emitters is shown in Fig. 5. For comparison, typical  $I$ – $V$  curves for three diamond-clad Si tips arrays including phosphor-doped, boron-doped, and undoped diamond-clad Si tips arrays are also shown in Fig. 5. The cathode for all these  $I$ – $V$  measurements consists of one unit of array with  $50 \times 50$  cells and each individual cell size is 3  $\mu\text{m}$  by 3  $\mu\text{m}$ . Typical surface morphology of an array of phosphor-doped diamond-clad Si tips is shown in Fig. 6. The details of process of these diamond-clad samples have been described previously.<sup>15</sup> Briefly, arrays of uncoated Si tips with tip radius of about 20 nm were used as templates for diamond cladding. However, diamond cladding results in a much blunter tip shape than the original uncoated Si tips.

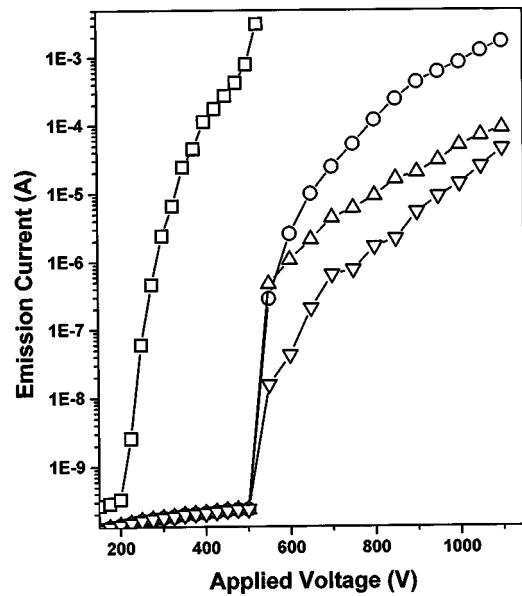


FIG. 5. Emission current vs applied voltage of an array with  $50 \times 50$  cells of CNT with symbol (□), P-doped diamond with symbol (○), B-doped diamond with symbol (△), undoped diamond with symbol (▽).

It is quite obvious that CNT emitters are more effective than diamond-clad Si tips. At an applied anode voltage of 525 V (i.e., an applied field of 17.5 V/ $\mu\text{m}$ ), a total emission current of 3.8 mA was achieved from an array of CNT emitters. In contrast, the corresponding emission current at the same applied voltage from all the diamond-clad Si tips arrays was only in the range of nA. Nevertheless, a comparable emission current can still be drawn from these diamond-clad Si tips arrays at somewhat higher applied voltages. For instance, at the maximum accessible voltage of 1100 V ( $\sim$  applied field of 36.7 V/ $\mu\text{m}$ ) in our setup, the emission currents were 1.69 mA, 90  $\mu\text{A}$ , and 45  $\mu\text{A}$  from arrays of phosphor-doped, boron-doped, and undoped diamond-clad Si tips, respectively. It should be noted that these emission currents are remarkable. If we assume that all the emissions

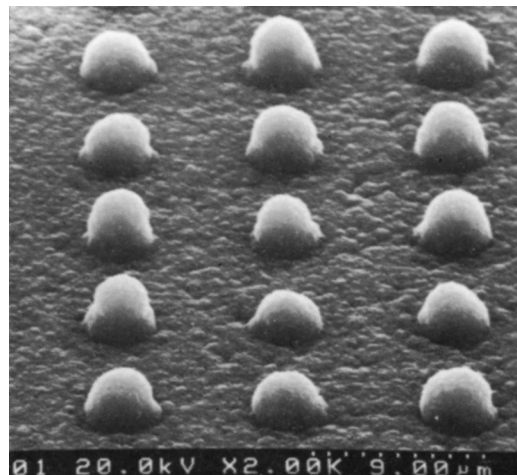


FIG. 6. SEM micrograph of an array of phosphor-doped diamond-clad Si tips.

occurred uniformly over the  $50 \times 50$  cells, the average ‘‘effective current density’’ (for CNT emitters at  $17.5 \text{ V}/\mu\text{m}$ ) could reach  $17 \text{ A}/\text{cm}^2$  since the effective emitting area is about  $2.25 \times 10^{-4} \text{ cm}^2$ . If we take the size of the array as the macroscopic emitting area, which is about  $2.5 \times 10^{-3} \text{ cm}^2$ , then the average macroscopic current density is  $1.5 \text{ A}/\text{cm}^2$  (for CNT emitters at  $17.5 \text{ V}/\mu\text{m}$ ). For convenience, macroscopic current density will be used hereafter.

A useful parameter for comparing the emission properties among various emitters is  $F_T$ , which is defined as the ‘‘threshold’’ value of the macroscopic field needed to generate a current density of  $10 \text{ mA}/\text{cm}^2$ , typical value required for effectively exciting a phosphor pixel in a field emission display. This current density is equivalent to a total current of  $25 \mu\text{A}$  in our case. The other parameter is  $F_o$ , which is defined as the macroscopic field to ‘‘turn on’’ a current density of  $10 \mu\text{A}/\text{cm}^2$ , equivalent to a total current of  $25 \text{ nA}$  in our case. The  $F_T$  value was  $33.6 \text{ V}/\mu\text{m}$  for the undoped diamond-clad Si tips and was reduced to  $30 \text{ V}/\mu\text{m}$  for the B-doped ones and  $22.3 \text{ V}/\mu\text{m}$  for the P-doped ones. The  $F_o$  values for the undoped, B-doped, and P-doped diamond-clad Si tips emitters were  $18.6$ ,  $15.5$ , and  $16.7 \text{ V}/\mu\text{m}$ , respectively. Compared with all the diamond-clad Si tips emitters, CNT emitters gave the lowest  $F_o$  and  $F_T$  values. With the four samples of CNT emitters, we find that the  $F_o$  and  $F_T$  values varied between  $5.8$ – $7.7$  and  $9.4$ – $11.3 \text{ V}/\mu\text{m}$ , respectively. These values are slightly higher than those reported for arc discharge samples.<sup>7–9</sup> In comparison to diamond-clad samples, the lower  $F_T$  and higher emission current of CNT emitters can be attributed to a large field enhancement factor due to their geometric characteristics and high conductivity of carbon nanotubes. The electron emission from P-doped diamond-clad Si tips exhibited enhanced emission property as compared to their B-doped and undoped counterparts. It is believed that the P dopants and their associated defect densities increase the energy state densities within the band gap of the diamond films,<sup>16,17</sup> leading to a higher conductivity and a remarkable enhancement of the electron emission.

Figure 7 depicts the corresponding Fowler–Nordheim plots of the emissions shown in Fig. 5. The linearity of the plot indicates that all the emitters follow the Fowler–Nordheim behavior. The slope and the intercept of FN plot depend on the values of work function ( $\phi$ ), field enhancement factor ( $\beta$ ), and emission area ( $\alpha$ ). In principle, if we know any one of the  $\phi$ ,  $\beta$ , and  $\alpha$  values, the other two values can be determined. However, these values are often difficult to estimate directly from FN equation due to the difficulty in determining the actual emission area, especially for cathode of irregular surface morphology such as tips and nanotubes. For CNTs, clear evidence of electrons emission from the end of tubes has been demonstrated recently by Zhu *et al.*<sup>13</sup> Emission from the surface of tube cylinder might not be excluded since its curvature is quite large, leading to substantial local field enhancement. Obviously, the values of  $\phi$  and  $\beta$  would be quite different at emission sites with different structure and geometric features. If, however, we assume  $\phi = 5 \text{ eV}$  as for graphite and  $C_{60}$  (Ref. 18) and  $\alpha$  value as the

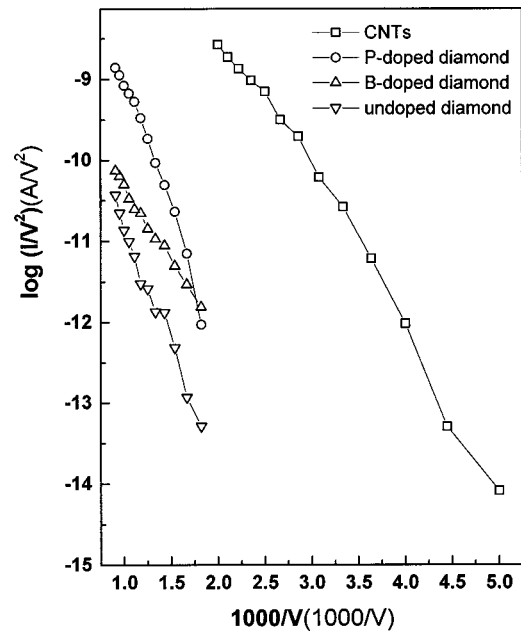


Fig. 7. FN plot for the data shown in Fig. 5 with CNT with symbol ( $\square$ ), P-doped diamond with symbol ( $\circ$ ), B-doped diamond with symbol ( $\triangle$ ), undoped diamond with symbol ( $\nabla$ ).

total cell area, a  $\beta$  factor of several thousands for the CNT emitters is obtained.

While the goal for drawing high electron emission current at low macroscopic field is achieved, the long-term stability is another important issue to be addressed. A way of testing emission stability is done by monitoring the temporal evolution of the emission current value ( $I$ ) compared with the initial emission current ( $I_0$ ) under a constant applied voltage. The  $I/I_0$  as a function of operation time for an array of CNT is shown in Fig. 8. The test was done at two different applied voltages. Figure 8(a) shows the  $I/I_0$  versus time at the maximum accessible voltage of  $1100 \text{ V}$ . The emission current dropped to  $60\%$  of the initial value in a few seconds and to only  $12\%$  after  $900 \text{ s}$  stress. The emission stability for CNT at stress voltage of  $1100 \text{ V}$  is rather poor in comparison to that of diamond-clad and carbon-coated Si tips<sup>19</sup> or that of

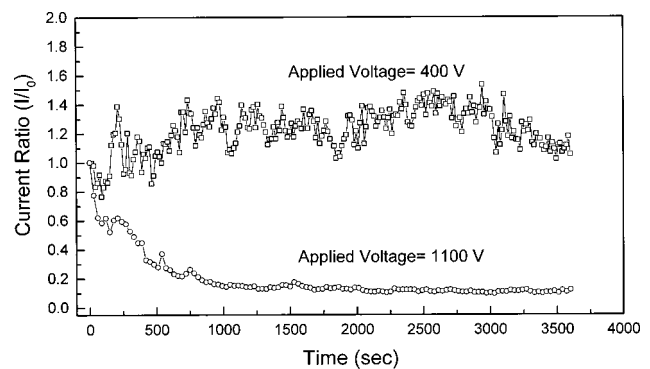


Fig. 8. Emission current ratio  $I/I_0$  vs stress time at an applied anode voltage of (a)  $1100 \text{ V}$  with symbol ( $\circ$ ) and (b)  $400 \text{ V}$  with symbol ( $\square$ ). The  $I_0$  value for case (b) was  $40 \text{ mA}/\text{cm}^2$ .

SiCN nanorods<sup>20</sup> at the same stress voltage. However, it should be pointed out that the stability measurement has not been standardized so far. Comparing  $I/I_0$  versus time at the same stress voltage does not have any physical meaning since the  $I_0$  values are different for different emitters. In our case for CNT sample, an operating condition near the maximum voltage of 1100 V ( $\sim 36.7$  V/ $\mu\text{m}$ ) is far away from its turn-on field (7.7 V/ $\mu\text{m}$ ) and its threshold field (11.1 V/ $\mu\text{m}$ ). The emission current at this voltage is enormous. Under such a high power stress, a rapid degradation in emission current can be expected. In fact, saturation and significant fluctuation of the emission current has occurred as we swept the anode voltage above 550 V ( $\sim 18.3$  V/ $\mu\text{m}$ ). The highest current we can obtain before saturation was about 3–4 mA ( $\sim 1.2$ – $1.6$  A/cm<sup>2</sup>).

The degradation in field emission performance can be largely accounted for by progressive destruction of CNT structure, presumably, due to poor adhesion between the CNT and the substrate as well as sustained ion bombardment of the tubes. The latter is attributable to gas phase electron ionization or ion desorption from the anode, both induced by the emitted electrons.<sup>11</sup> Obviously, the decay characteristics will be very different if we choose another test condition such as a voltage around threshold. Figure 8(b) shows the  $I/I_0$  versus time at 400 V ( $\sim 13.3$  V/ $\mu\text{m}$ ). The macroscopic current density at this point was about 40 mA/cm<sup>2</sup>. Although some fluctuation in the emission current was observed, there was no sign of degradation during the testing period. The emission stability at this high current density is promising for practical application in flat panel display. Further investigation on the operating condition to maintain long term stability of CNT is underway.

#### IV. CONCLUSIONS

Arrays of carbon-based emitters with well-separated cells of  $\mu\text{m}$  scale have been fabricated and their field emission properties have been characterized. CNT grew only on top of the metal layer in the array but not on the plain Si substrate. The fabrication process of patterned template is well established and is applicable for large area process. Subsequent deposition of catalytic metal layer and growth of CNT or diamond cladding involves e-beam evaporation and CVD, all of which are also quite straightforward. Hence, our synthetic approach is well within the capabilities of the current IC industry for automation and scale up production of practical devices.

The carbon nanotubes grown by MWCVD were 20–30  $\mu\text{m}$  in length and 60–70 nm in diameter. The density of CNT within each cell was very high while no tube growth outside the catalytic cells was found. Field emission investigation reveals high emission current at low voltage for these

samples. To draw a macroscopic current density of 10  $\mu\text{A}/\text{cm}^2$  and 10 mA/cm<sup>2</sup>, the macroscopic electric fields required (defined as the turn-on and threshold field) for carbon nanotubes were 5.8–7.7 and 9.4–11.3 V/ $\mu\text{m}$ , respectively. Much higher fields were required to give emission currents of comparable values from arrays of phosphor-doped, boron-doped and undoped diamond-clad Si tips. Macroscopic emission current density in excess of 1 A/cm<sup>2</sup> can be achieved with moderate applied fields ( $\sim 17$ – $18$  V/ $\mu\text{m}$ ) from arrays of CNT emitters. Furthermore, emission stability at high current density (several tens of mA/cm<sup>2</sup>) of the CNT emitters offers promising future for vacuum microelectronic applications.

#### ACKNOWLEDGMENTS

The research was supported in part by the National Science Council in Taiwan under the Contract Nos. NSC 88-2112-M002-022, NSC 89-2112-M002-047, and NSC 87-2215-E009-052. Technical supports from the National Nano Device Laboratory of NSC and Semiconductor Research Center of National Chiao-Tung University are also acknowledged.

<sup>1</sup>P. Vaudaine and R. Meyer, IEEE IEDM Tech. Dig., 197 (1991).

<sup>2</sup>H. H. Busta, J. E. Pogemiller, and B. J. Zimmerman, J. Micromech. Microeng. **3**, 45 (1993).

<sup>3</sup>T. H. P. Chang *et al.*, J. Vac. Sci. Technol. B **9**, 438 (1991).

<sup>4</sup>C. A. Spindt, Surf. Sci. **266**, 145 (1992).

<sup>5</sup>K. Okano, S. Koizumi, S. R. P. Silva, and G. A. J. Amaratunga, Nature (London) **381**, 140 (1996).

<sup>6</sup>M. W. Geis, J. C. Twichell, N. N. Efremion, K. Krohn, and T. M. Lyszczarz, Appl. Phys. Lett. **68**, 2294 (1996).

<sup>7</sup>W. A. de Heer, A. Chatelain, and D. Ugarte, Science **270**, 1179 (1995).

<sup>8</sup>P. G. Collins and A. Zettl, Appl. Phys. Lett. **69**, 1969 (1996).

<sup>9</sup>Q. H. Wang, T. D. Corrigan, J. Y. Dai, and R. P. H. Chang, Appl. Phys. Lett. **70**, 3308 (1997).

<sup>10</sup>Z. F. Ren, Z. P. Huang, J. W. Xu, J. H. Wang, P. Bush, M. P. Siegal, and P. N. Provencio, Science **282**, 1105 (1998).

<sup>11</sup>J.-M. Bonard, J.-P. Salvetat, T. Stockli, W. A. de Heer, L. Forro, and A. Chatelain, Appl. Phys. Lett. **73**, 918 (1998).

<sup>12</sup>O. M. Küttel, O. Groening, C. Emmenegger, and L. Schlapbach, Appl. Phys. Lett. **73**, 2113 (1998).

<sup>13</sup>W. Zhu, C. Bower, O. Zhou, G. Kochanski, and S. Jin, Appl. Phys. Lett. **75**, 873 (1999).

<sup>14</sup>S. Fan, M. G. Chapline, N. R. Franklin, T. W. Tombler, A. M. Cassell, and H. Dai, Science **283**, 512 (1999).

<sup>15</sup>T. K. Ku, S. H. Chen, C. D. Yang, N. J. She, C. C. Wang, C. F. Chen, I. J. Hsieh, and H. C. Cheng, IEEE Electron Device Lett. **17**, 208 (1996).

<sup>16</sup>G. B. Bachelet, G. A. Baraff, and M. Schlüter, Phys. Rev. B **24**, 4736 (1981).

<sup>17</sup>W. Zhu, G. P. Kochanski, S. Jin, and L. Seibles, J. Appl. Phys. **78**, 2707 (1995).

<sup>18</sup>B. Robrieux, C. R. Acad. Sci. **278**, 659 (1974).

<sup>19</sup>P. D. Kichambare, F. G. Tarntair, T. Y. Wang, L. C. Chen, K. H. Chen, and H. C. Cheng, J. Vac. Sci. Technol. B (to be published).

<sup>20</sup>K. H. Chen, J.-J. Wu, L. C. Chen, C. Y. Wen, P. D. Kichambare, F. G. Tarntair, P. F. Kuo, S. W. Chang, and Y. F. Chen, Diamond Relat. Mater. **9**, 1249 (2000).